

LEVEL II

DEPARTMENT OF THE NAVY
United States Naval Academy
Annapolis, Maryland 21402

(5)

Division of Engineering and Weapons

AD A110883

Report No. EW-12-81

DYNAMIC RESPONSE OF HOVERCRAFT LIFT FANS

David D. Moran*

August 1981

DTIC
ELECTE
FEB 12 1982
S **D**
H

Approved for public release

Distribution Unlimited

*NAVSEA Research Professor
Naval Systems Engineering Department
U. S. Naval Academy
Annapolis, Maryland

DTIC FILE COPY

820-11-11

DEPARTMENT OF THE NAVY
United States Naval Academy
Annapolis, Maryland 21402

Division of Engineering and Weapons

Report No. EW-12-81

DYNAMIC RESPONSE OF HOVERCRAFT LIFT FANS

David D. Moran*

August 1981

Approved for public release
Distribution Unlimited

*NAVSEA Research Professor
Naval Systems Engineering Department
U. S. Naval Academy
Annapolis, Maryland

Accession For	
DTIC	
DTIC	
USCIB	
DTIC	
By	
Date	
Avail	
Dist	
A	

DYNAMIC RESPONSE OF HOVERCRAFT LIFT FANS

SYNOPSIS

Hovercraft lift fans are subjected to varying back pressure due to wave action and craft motions when these vehicles are operating in a seaway. The oscillatory back pressure causes the fans to perform dynamically, exhibiting a hysteresis type of response and a corresponding degradation in mean performance. Since hovercraft motions are influenced by variations in lift fan pressure and discharge, it is important to understand completely the nature of the dynamic performance of lift fans in order to completely solve the hovercraft seakeeping problem.

The present study was performed to determine and classify the instabilities encountered in a centrifugal fan operating against time-varying back pressure. A model-scale experiment was developed in which the fan discharge was directed into a flow-measuring device, terminating in a rotating valve which produced an oscillatory back pressure superimposed upon a mean aerodynamic resistance. Pressure and local velocity were measured as functions of time at several locations in the fan volute. The measurements permitted the identification of rotating (or propagating) stall in the impeller. One cell and two cell configurations were classified and the transient condition connecting these two configurations was observed. The mechanisms which lead to rotating stall in a centrifugal compressor are presented and discussed with specific reference to hovercraft applications.

INTRODUCTION

The lift fans of a hovercraft operating in a seaway are subjected to temporally varying back pressure due to the combined effects of wave action and craft motions. Oscillatory back pressure causes the lift fans to respond dynamically under unsteady flow conditions and often to exhibit a hysteresis type of response in the discharge. This phenomenon has been observed experimentally by several investigators including Greitzer¹ and Durkin². An extensive survey of the literature on this subject prior to 1978 has been previously published by Moran and Bullock³.

Craft motions are influenced by variations in lift fan pressure and discharge. It is therefore important to achieve an understanding of the dynamic response of lift fans since the performance hysteresis can cause significant deviations from the static fan operating curve. During the design of a lift fan, performance is usually considered only for steady flow conditions since no general analytical tools are available to the designer to predict fan dynamic response. A full understanding of fan dynamic response is needed to develop these analytic

tools for fan design and to determine the effect of fan response on craft motions.

The goal of the present investigation was to determine the types of instabilities that occur in a typical centrifugal lift fan while operating against varying back pressure and to relate these instabilities to fan dynamic response. Specifically, the purpose of the present experimental investigation was to:

1. Develop a procedure (equipment and methods of analysis) to identify the incidence of propagating stall as a major dynamic characteristic of hovercraft lift fans.
2. Develop methods to quantify the phenomenon in terms of velocities, pressures, and rotational rates.
3. Determine the external conditions (unsteady backflow) under which a specific fan would exhibit propagating stall.
4. Examine the interactive effect of the stall phenomenon on the dynamic performance characteristics of the fan system.

The two types of instabilities that commonly occur in axial and centrifugal compressors are surge and rotating stall. Surge is a Helmholtz-type resonance characterized by large changes in mass flow rate, reverse flow, and often severe mechanical vibration of the compressor. Generally, surge is accompanied by simultaneous stall on all rotor blades. Average mass flow rate over the entire rotor is therefore time dependent. Rotating stall, on the other hand, displays two characteristics significantly different from those of surge. First, a fan operating with rotating stall will usually have a constant mass flow rate averaged over the entire rotor. And second, the fan blades are not subject to simultaneous stall but rather stall in some orderly fashion. Spontaneous surge was not generated in this experiment and hence the discussion is directed solely towards examination of the rotating stall phenomenon.

Propagating or rotating stall occurs when one or more regions of stall propagate around the rotor at some frequency, ω_s , different from the fan frequency, ω_f . The mechanism of rotating stall may be described as follows. Assume that a transient disturbance causes one blade of an unstalled rotor to stall. This restricts the flow through the passage between the stalled blade and the next blade in line. If the pressure remains essentially constant then the local flow must change due to stall cell blockage. The effect of the diverted flow is to increase the angle of attack, α , on the next blade in line in the tangential direction of inlet velocity, and to lower α in the opposite direction, that is, on the preceding blade. Stall occurs on the next blade due to increased α and the process continues. After stall has propagated some distance, the incident angle on the first blade decreases, and the flow reattaches (i.e., the blade is no longer stalled). Reattachment occurs as the stalling of succeeding blade passages diverts some flow in the direction to decrease the angle of attack on the first stalled blade. Rotating stall can occur with various numbers of cells and cell sizes depending upon the characteristics of the individual rotor, speed of propagation, and external excitation. Propagating stall is often evident during surge and may precipitate the latter (see Emmons, et al⁴). Mild surge is often accompanied by prolonged bursts of rotating stall. The cause-effect relationship is not presently understood but is most certainly related to the non-homogeneous surge-generated stall on blades

at various positions in a non-prismatic volute. One might expect to find stall regions moving at a velocity which is associated with the rate of formation and recovery of separation regions and, hence, ω_s is certainly dependent upon the individual fan geometry.

BACKGROUND

Work in the area of unsteady compressor performance has been going on for several years, primarily with axial compressors and to a lesser extent centrifugal compressors. Compared to the common hovercraft lift fan these centrifugal compressors have more blades and typically produce a larger pressure rise for the equivalent discharge. Some observations of earlier experimenters which are relevant to this investigation are reviewed in this section, and correlation of their observations with those made in this study is discussed in a later section.

Emmons, et al⁵ have noted that for a centrifugal compressor both surge and rotating stall could occur. The authors observed a 3 cell stall configuration propagating at a frequency ω_s equal to $0.25 \omega_f$. In a later investigation on an axial compressor, Emmons, et al⁴ noted that rotating stall could precipitate surge, and further noted that an analytical model would require non-linear, non-steady theory to describe surge or rotating stall.

Working with an axial compressor, Rockett⁶ noted a transient phenomenon occurring at irregular intervals involving changes in the spacing of stall cells. This phenomenon typically preceded a change in the number of stall cells. Propagation rate was seen to be a function of cell configuration. The author also observed a small dependency of cell propagation rate upon compressor mass flow.

Lennemann⁷ investigated rotating stall in both shrouded and unshrouded centrifugal compressors. He concluded that stall propagation was a process of boundary layer separation which is strongly influenced by secondary flows in the rotor. This would help to explain the range of propagation rates reported in the literature since secondary flows are closely related to compressor geometry.

In an investigation on an axial compressor, Greitzer¹ reported rotating stall propagating at 0.25 to 0.3 times the rotor frequency. He also determined that the dynamic response of the compressor system showed a Helmholtz dependency. The implication of this observation is that the gross dynamic response of a fan is closely linked to acoustic properties of the system in which the fan is being operated.

Amann, et al⁸ investigated unsteady performance of a centrifugal compressor. It was noted that the propagation speed of the stall cells increased with both an increase in discharge, Q , and a decrease in rotational rate of the fan. The observation that rotating stall occurred prior to and during surging of the compressor was also reported by these investigators.

EXPERIMENTAL PROCEDURES

In order to examine propagating stall in a centrifugal flow fan typical of those employed in hovercraft lift systems, a fan test facility⁹ was developed by the DTNSRDC Ship Performance Department. Using this facility, an experimental study of fan dynamics was undertaken on a model fan. Specific experiments were performed with a 1/6 scale model of a lift fan designed for the U. S. Navy Amphibious Assault Landing Craft Program and have been reported by Jennings and Moran¹⁰. The model scale rotor is a 12 bladed centrifugal fan with high efficiency backward curved airfoil blades having a 45° exit angle. A description of the rotor, volute, inlet, and diffuser is given by Jennings and Turner¹¹. The model fan discharged into an 8 inch diameter pipe in which volumetric flow was measured. The pipe exit was fitted with a rotary valve which could be used to develop a periodic back pressure and associated periodic discharge. The valve frequency, ω_v , could be varied between 0 and 10 Hz. A schematic of the experimental setup is shown in Figure 1.

The fan facility and fan volute were extensively instrumented. Velocity and pressure measurements were taken in the volute. Pressure measurements included those at the inlet, volute, exit, along the volute spiral at $\theta = 120^\circ$, on the back side of the volute at $\theta = 240^\circ$, and along the volute spiral at $\theta = 240^\circ$, where θ is measured in the direction of fan rotation with origin at the volute lip. All pressures were sensed by flush-mounted pressure taps. Velocity measurements were made with constant temperature hot wire anemometers. These two probes were located next to the rotor blade exit. Placement of the velocity probes was varied during the experiment to include the following three sets of angular locations: 120° and 240°, 120° and 150°, and 15° and 345°.

Time histories of each of the test variables were recorded on magnetic tape. Signals on the data tape were displayed on an oscillograph recorder for inspection and analysis of the time histories. Each run was also digitized, and both auto spectra and cross spectra were computed by Fast Fourier Transform techniques to determine the frequency content of each signal.

The experimental program was designed to identify and examine propagating stall through variations in control conditions. The fan was tested at various fan rotational rates between 5500 and 9000 rpm, and the valve frequency, ω_v , was varied from 0 to 8 Hz. The rotary valve was constructed so that, when fully closed, 92% of the cross sectional area of the pipe was blocked, thus allowing some fan discharge at all times.

PRESENTATION AND DISCUSSION OF RESULTS

Rotating stall was observed during the experiment for all valve frequencies, ω_v , investigated including fixed or stationary valve positions of 0 Hz. Initiation of rotating stall occurred when the volute exit area had been reduced by 80% for cases where $\omega_v < 4$ Hz. When ω_v was greater than 4 Hz, system dynamics began to influence gross fan response, and the flow area blockage required to initiate rotating stall varied with valve frequency. In cases with $\omega_v > 0$ the fan was cycled from a

high discharge operating point to a low discharge operating point. During the low discharge portion of the cycle, rotating stall was observed. A typical example of the valve cycle is shown in Figure 2 for $\omega_v = 0.69$ Hz ($\omega_f = 145$ Hz), and it is instructive to examine this time history in detail. As the valve closes, pressure in the fan gradually increases and flow rate decreases. At the point in time designated as EVENT A, unsteady behavior is detected along with a small but distinct drop in measured pressure and an increase in mean velocity. Further closure of the valve causes the larger periodic fluctuations in pressure shown as EVENT B and the velocity characteristic of rotating stall. As the valve opens, rotating stall ceases to occur at EVENT C and more unsteady transition behavior is observed before the fan returns to a steady state type of operation noted as EVENT D.

For the runs with $\omega_v = 0$ and the pipe flow area reduced by at least 80%, the same type of pressure and velocity time histories were recorded as in the rotating stall portion of the valve cycle. An example of this behavior is shown on an expanded time scale in Figure 3. This example represents a fan operating at a rotational rate of $\omega_f = 124$ Hz which yields a blade rate frequency of $\omega_b = 1488$ Hz. The periodic disturbance shown at a frequency of $\omega_s = 62$ Hz represents a one-cell rotating stall configuration rotating at roughly one half of the fan rotational rate, $\omega_s/\omega_f = 0.5$. The blade rate frequency cannot be clearly seen in this figure but is implied by the high frequency signal superimposed upon the stall cell velocity periodicity shown in the blade exit velocity time histories. The periodicity in inlet pressure is not caused by surge but is the same as that shown between EVENTS B and C in Figure 2.

The time dependent back pressure generated by valve rotations is accompanied by a variation in the operating point for the fan. A measure of the variation was obtained simultaneously with the detailed time histories. As previously mentioned, under conditions of dynamic excitation a fan does not operate on the steady state curve but exhibits a hysteresis response. The loop associated with a valve frequency of $\omega_v = 0.48$ Hz is shown in Figure 4. Also shown is the steady state operating curve for the test fan. As ω_v increases, larger and more rapid changes in pressure are observed with smaller changes in flow rate. The exact shape of the hysteresis loop is dependent upon fan and system dynamic characteristics, the fan dynamics being associated with rotating stall.

An interesting feature of this figure is the fact that, locally, pressures may be raised above the static operating curve when the fan is operated dynamically. This is caused by the effective storage and release of energy in the volute due to compressibility, but it does not make the fan more efficient. Fan efficiency, defined as the product of pressure and discharge divided by the shaft power, is less for periodic excitation than for static operation due to higher shaft power requirements. Unsteady shaft power can be measured and correlated with results such as those shown in Figure 4.

Examination of the effects of propagating or rotating stall in past engineering applications has been impeded by lack of a clear methodology of stall classification. One accomplishment of this experimental program was the development of a method of identifying propagating stall and the

conditions which lead to its formation. This was achieved through analysis of the velocity fields near the blades which were measured with at least two spatially separated hot wire anemometers. Characteristics of a particular stall cell were identified at the first probe location and later at the second probe location. Knowing the rotor speed, stall frequency and stall cell size could be measured from the time histories.

Two distinct stall patterns were identified throughout the test. One pattern was a two-cell configuration, each cell propagating at a rotational frequency given (approximately) by $\omega_s = 0.65 \omega_f$. The second configuration was a single cell propagating at a frequency in a range of $0.48 \omega_f$ to $0.53 \omega_f$. This dependence on stall cell configuration for propagation rate relative to rotor speed was consistent with observations of Rockett⁶. The measured variations in ω_s were small and did not show any distinct relationship to flow rate (as⁵ was noted by Rockett⁶), rotor rotational speed, or the valve rotational speed. Interestingly, the ratio ω_s/ω_f was nearly constant with each cell configuration for values of ω_f ranging from 5500 rpm to 9000 rpm. This same observation was also reported by Emmons et al³ and Greitzer¹. Although not conclusive, it suggests that the stall cell velocity is independent of the rotor Reynolds number over some range of Reynolds number.

Spectral analysis of the time histories was performed to examine the frequency content and phase relationships of the signals. The major peaks in the power spectral density plots correlated well with the frequencies determined from time histories. Figure 5 shows a sample plot of the power spectral density obtained from a hot wire probe located at $\theta = 240^\circ$ for $\omega_s = 0.93$ Hz. The fan rotational frequency is clearly seen at $\omega_f = 0.85 \times 10^3$ rad/sec ($\omega_f = 135$ Hz). Higher harmonics of this fan rate are also evident as small peaks at equal frequency spacings in the high frequency range. The frequencies of the two rotating stall configurations are indicated by the major peaks in the figure. The first, or left hand, peak represents a one-cell configuration with a stall cell velocity determined by $\omega_s/\omega_f = 0.50$. The right hand peak represents a two-cell propagating stall configuration rotating at a speed equal to 0.65 times the fan rotational rate (e.g., two cells with $\omega_s/\omega_f = 1.3$). The two configurations do not occur simultaneously, but they are both present at various times during the valve cycle. Since the process of spectral analysis requires a protracted time history, all dynamic characteristics of the system exist in the data record. As a final observation relating to Figure 5, the blade frequency associated with this particular experiment was $\omega_b = 10.2 \times 10^3$ rad/sec and therefore does not appear as a spike in the frequency range presented.

Cross spectral analysis was also performed with the data to determine the phase characteristics between pressures or velocities at different locations in the fan system while rotating stall was occurring. The small variations in ω_s combined with a high level of ambient turbulence in the volute and a seemingly arbitrary change of stall cell configuration often produced a low correlation between any two signals and hence poor phase information from the analyzed cross spectra. However, for steady discharge ($\omega_v = 0$), when sufficient run time was recorded and the aforementioned problems were less severe, phase angles from cross spectra correlated well with those determined from analysis of the time histories. In general it was found that analysis of the time histories

provided a more reliable determination of the phase angle between any two signals.

A detailed example of the development of a set of rotating stall cells is presented in Figure 6. When the exit valve is open (see Trace 6A) the fan is operating under ideal conditions and the signal trace indicates uniformity of the flow velocity from blade to blade. Individual blade passages are clearly seen in this velocity trace. As the valve begins to choke the flow, the velocity signal changes to that of Trace 6B. Here, perturbations in the velocity field begin to obscure blade passages. The dominant frequency indicates that every other blade shows some degree of stall. Further closure of the valve triggers a transition stage shown by Trace 6C between uniform operation and rotating stall. This portion includes different configurations of unsteady rotating stall rapidly being established and destroyed. Traces 6D and 6E show the velocity signals corresponding to $\omega_s = 1.3 \omega_f$ and $\omega_s = 0.5 \omega_f$, respectively. The fan was found to change between one and two-cell configurations during the course of some valve cycles. An example of such a cell transition is presented in Figure 7 where transition from a one-cell to a two-cell configuration is seen. These signals are a small portion of a run with $\omega_v = 0$. Changes in stall configuration normally occurred at irregular intervals. In the present case, when the valve was nearly shut, the configuration with $\omega_s = 1.3 \omega_f$ was the dominant frequency (in terms of length of time of occurrence). Neither configuration was clearly dominant when the valve was completely closed.

SUMMARY

The present study was performed to develop methodology for the determination and classification of flow instabilities encountered in a centrifugal hovercraft lift fan operating against an unsteady back pressure. A model-scale experimental procedure was developed and an experiment performed to study, specifically, the occurrence of propagating or rotating stall on the fan rotor. Hot wire anemometers were used as a primary tool in developing the method for identifying rotating stall. It was determined that the particular fan exhibits rotating stall with one and two-cell configurations without surge in the flow system. The unsteady aerodynamics of rotating stall includes different values of ω_s/ω_f for each rotating stall cell pattern. In addition, even for a given cell pattern small variations in ω_s/ω_f occurred. Also found in this system were spontaneous changes from a one-cell to a two-cell configuration, and the reverse, for a given operational mode. Rotating stall was excited when the exhaust area for the fan was reduced by 80% for $\omega_v = 0$, and was found for all values of $\omega_v > 0$. The effect of rotating stall on the dynamic performance of the test fan was not great, but some loss in fan pressure was measured when rotating stall was initiated.

ACKNOWLEDGMENTS

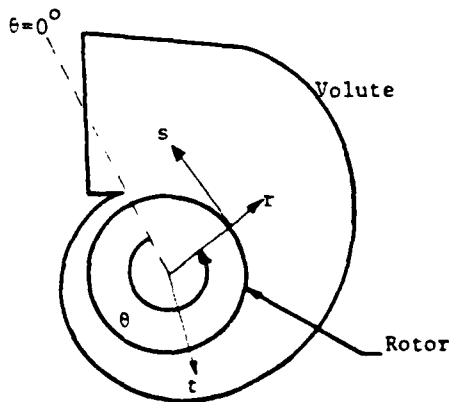
This report serves as the basis of a presentation to be read before the Third International Hovercraft Conference, Southampton, United Kingdom, November 1981, entitled "Dynamic Stall in Hovercraft Lift Fans" and authored by Alan N. Jennings, Margaret V. Bullock and the present author. Grateful acknowledgment is made to Mr. Jennings and Ms. Bullock for their contributions to this presentation.

REFERENCES

- 1) GREITZER, E.M. 1974, "Surge and Rotating Stall in Axial Flow Compressors" American Society of Mechanical Engineers Paper No. 75-GT-10
- 2) DURKIN, J.M., LUEHR, L.W.H. 1978, "Dynamic Response of Lift Fans Subject to Varying Back Pressure" AIAA/SNAME Advanced Marine Vehicles Conference
- 3) MORAN, D.D., BULLOCK, M.V. 1977, "Dynamic Response of Lift Fans Employed in Hovering Craft: A Review of the Literature" Hovering Craft and Hydrofoil, Vol. 16, No. 7-8
- 4) EMMONS, H.W., KRONAUER, R.E., ROCKETT, J.A. 1959, "Survey of Stall Propagation - Experiment and Theory" Trans. ASME, Vol. 2, Series B
- 5) EMMONS, H.W., PEARSON, C.E., GRANT, H.P. 1955, "Compressor Surge and Stall Propagation" Trans. ASME, Vol. 2, Series B
- 6) ROCKETT, J.A. 1959, "Modulation Phenomena in Stall Propagation" Trans. ASME, Vol. 2, Series B
- 7) LENNEMANN, E., HOWARD, J.H.G. 1969, "Unsteady Flow Phenomena in Rotating Centrifugal Impeller Passages" ASME Gas Turbine Conference
- 8) AMANN, C.A., NORDENSON, G.E., SKELLENGER, G.D. 1977, "Casing Modification for Increasing the Surge Margin of a Centrifugal Compressor in an Automotive Turbine Engine" ASME Gas Turbine Conference
- 9) JENNINGS, A.N. 1979, "Flow Measurement Facility Documentation" DTNSRDC Report SPD-0871-01
- 10) JENNINGS, A.N., MORAN, D.D. 1981, "Observations of Propagating Stall in a Centrifugal Fan" DTNSRDC Report SPD-0987-01
- 11) JENNINGS, A.N., TURNER, C. 1980, "Performance Test of the 1/6 Scale Model of the Original JEFF (A) Lift Fan" DTNSRDC Report SPD-0913-01

NOTATION

$A = \pi bd$	Rotor exit area
b	Blade exit width
d	Rotor diameter
N	Fan rotational rate
n	Number of stall cells around impeller
P	Fan exit pressure
Q	Volumetric discharge
r	Radial coordinate
s	Tangential coordinate
t	Normal coordinate
$u = \frac{\pi}{60} dN$	Fan tip speed
α	Angle of attack
ρ	Mass density
θ	Angular coordinate in fan volute
$\phi = \frac{Q}{Au}$	Discharge coefficient
$\psi = \frac{P}{\rho u^2}$	Pressure coefficient
ω_b	Blade rate rotational frequency
ω_f	Rotor rotational frequency
ω_s	Stall cell rotational frequency
ω_v	Rotary valve rotational frequency



t is normal to the page in the right-handed coordinate system r - s - t . s is shown at the value of r corresponding to the blade exit. Angular measurements are made from the volute exit lip.

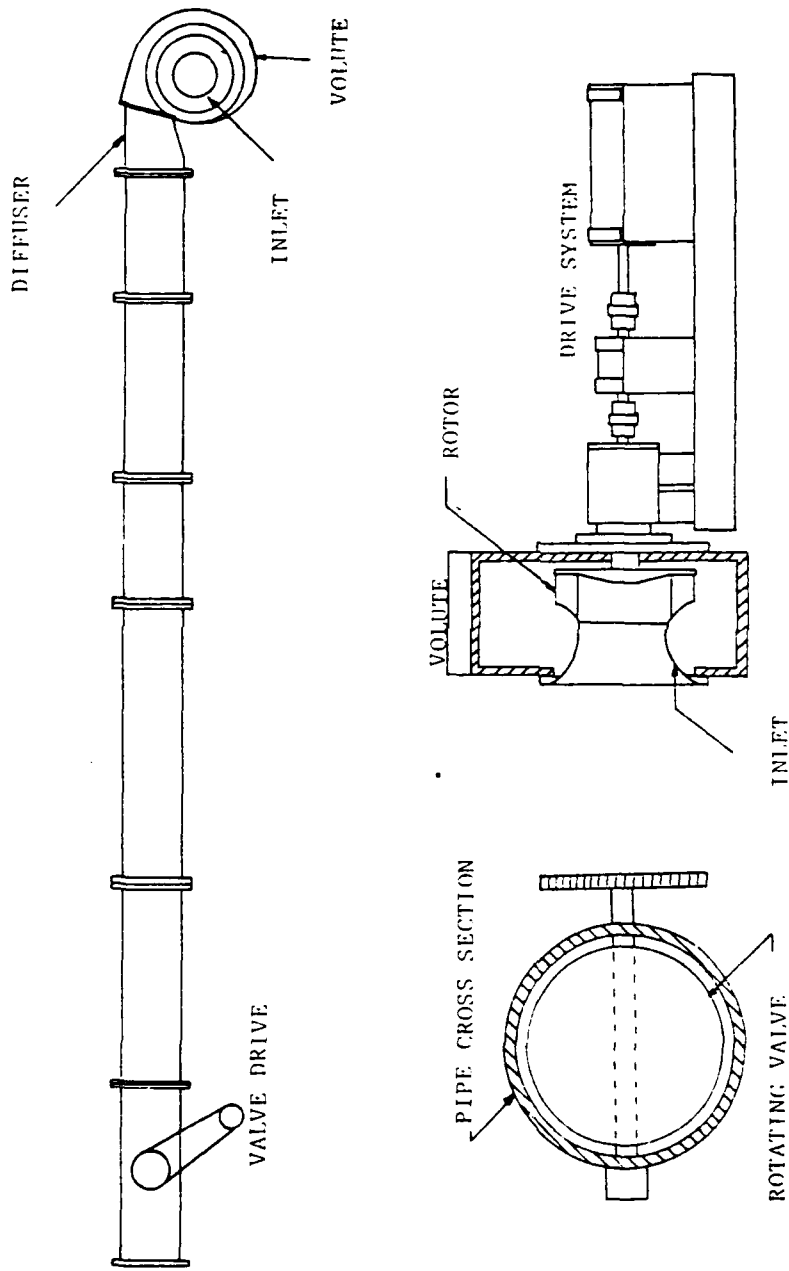


Figure 1 - Experimental Equipment

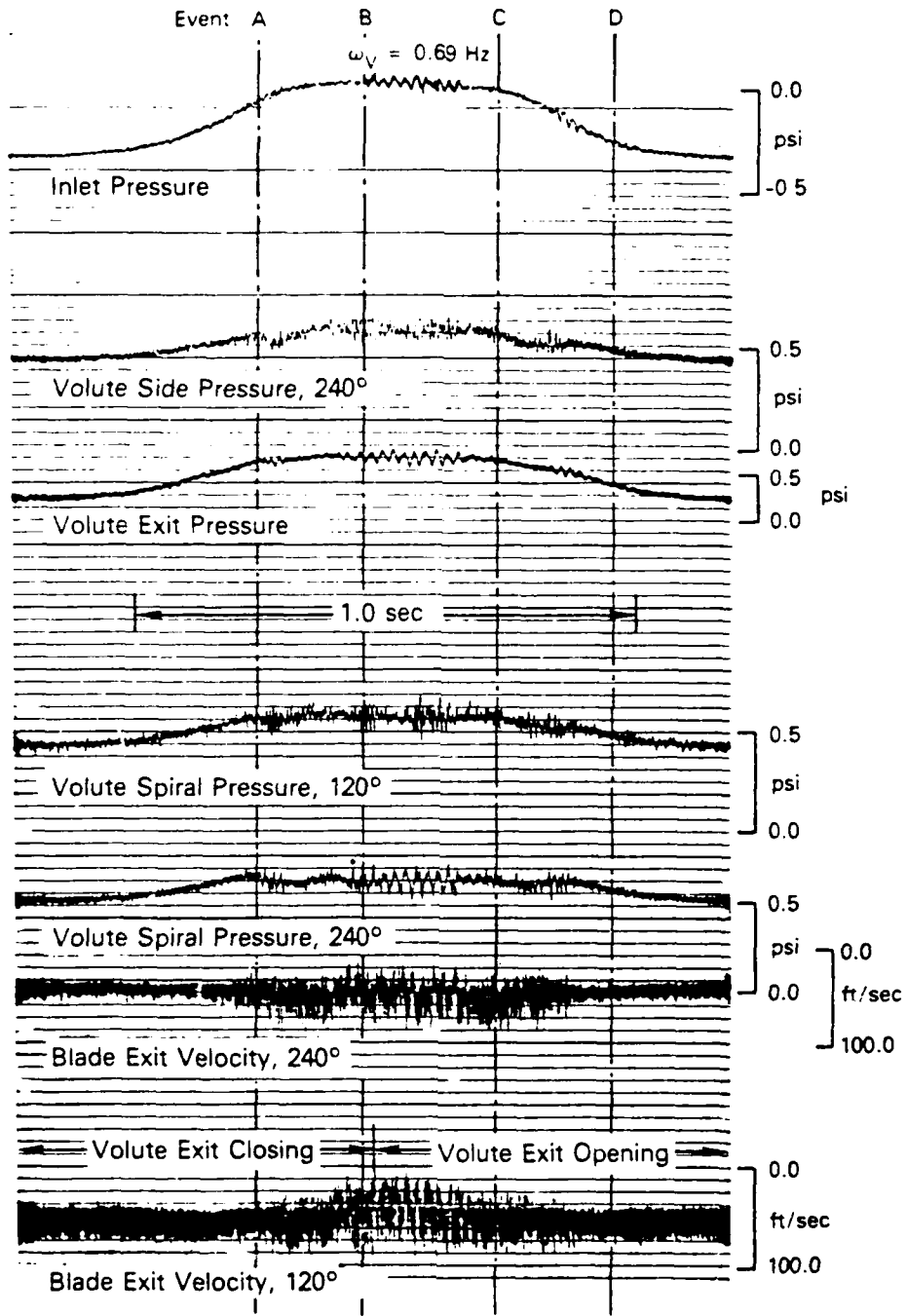


Figure 2 - Typical Time History of One Valve Cycle for $\omega_V = 0.69 \text{ Hz}$

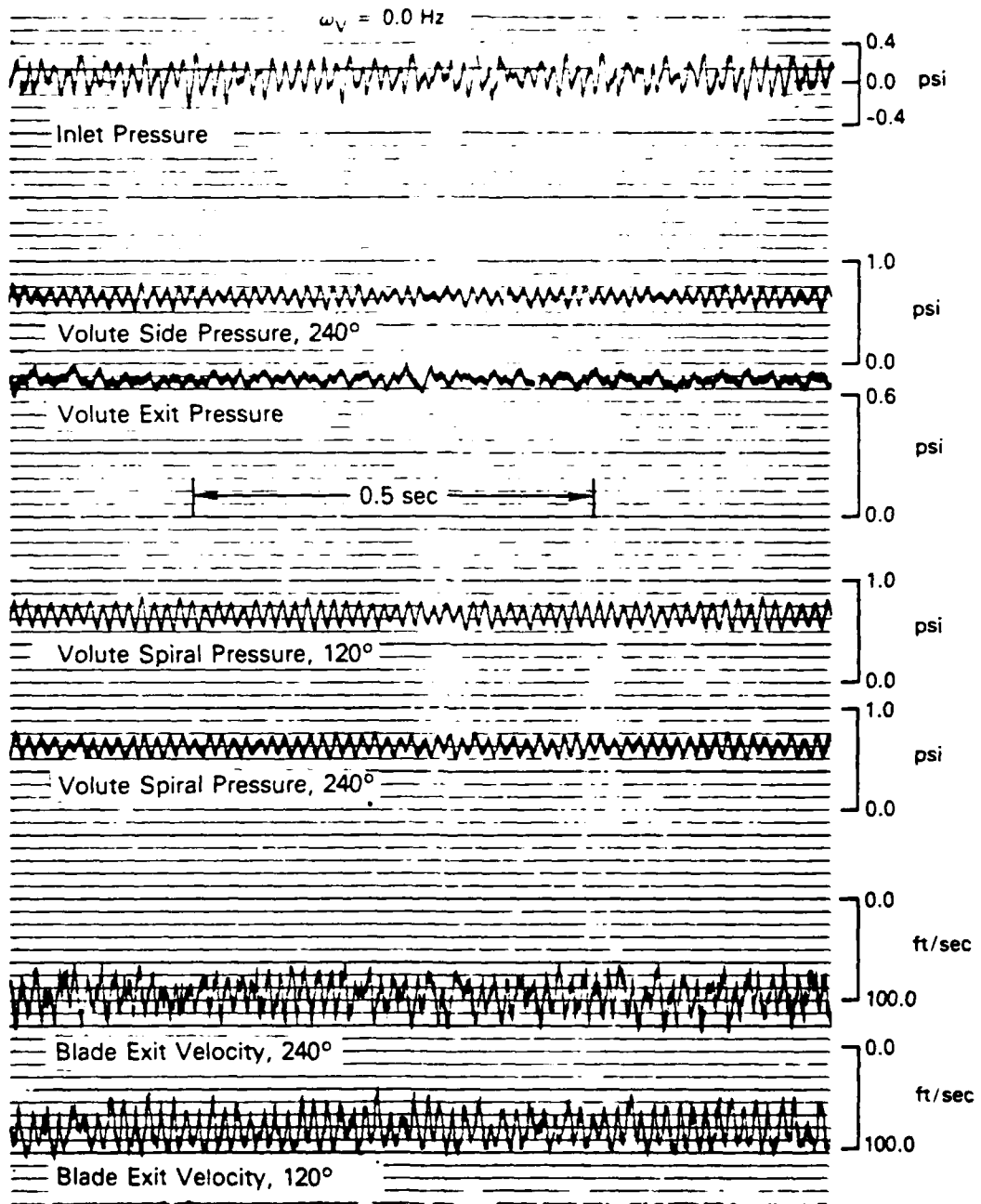


Figure 3 - Typical Time History for $\omega_v = 0$

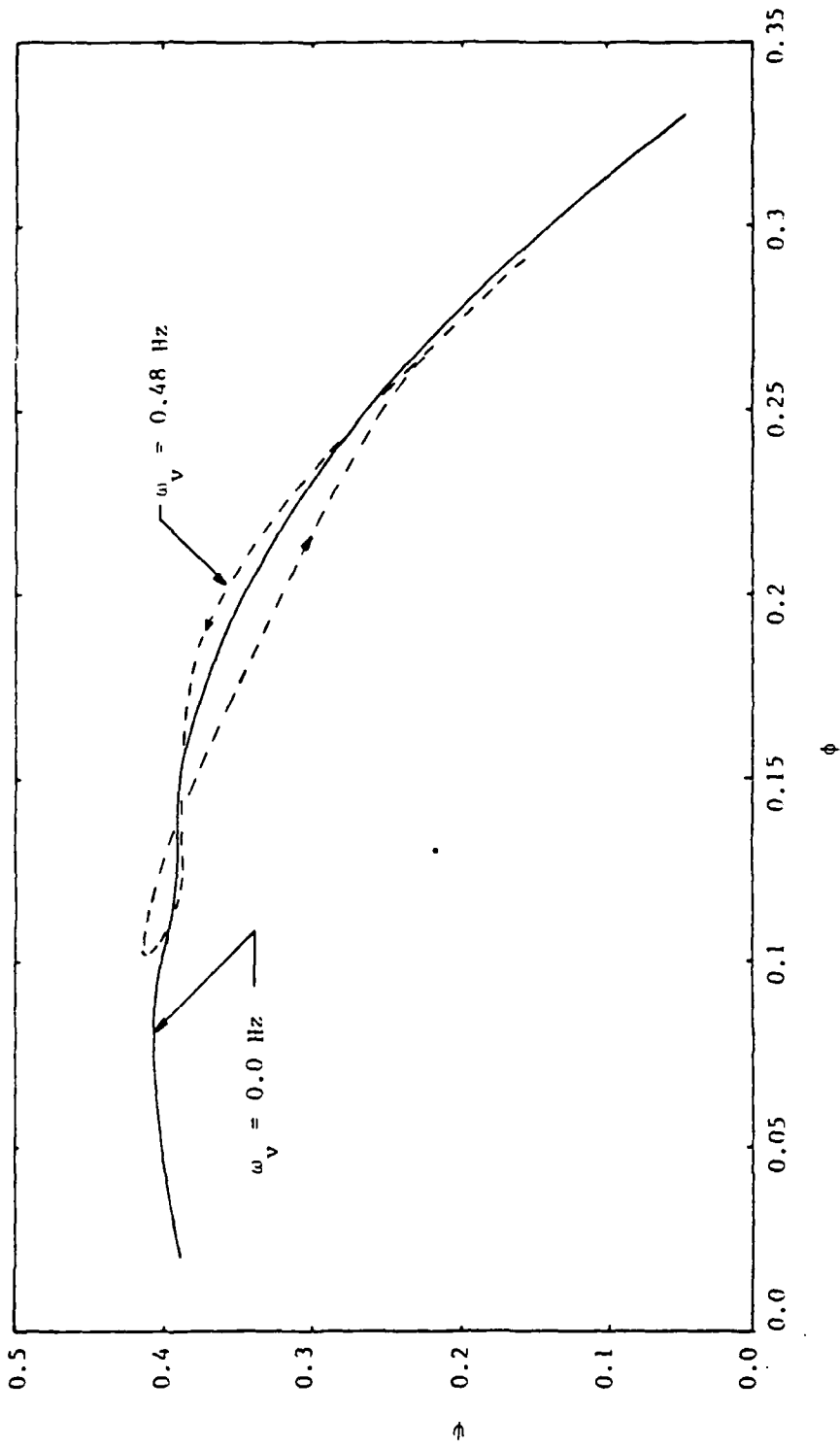


Figure 4 - Comparison of Fan Dynamic Response at $\omega_v = 0.48$ Hz with Static Operating Curve

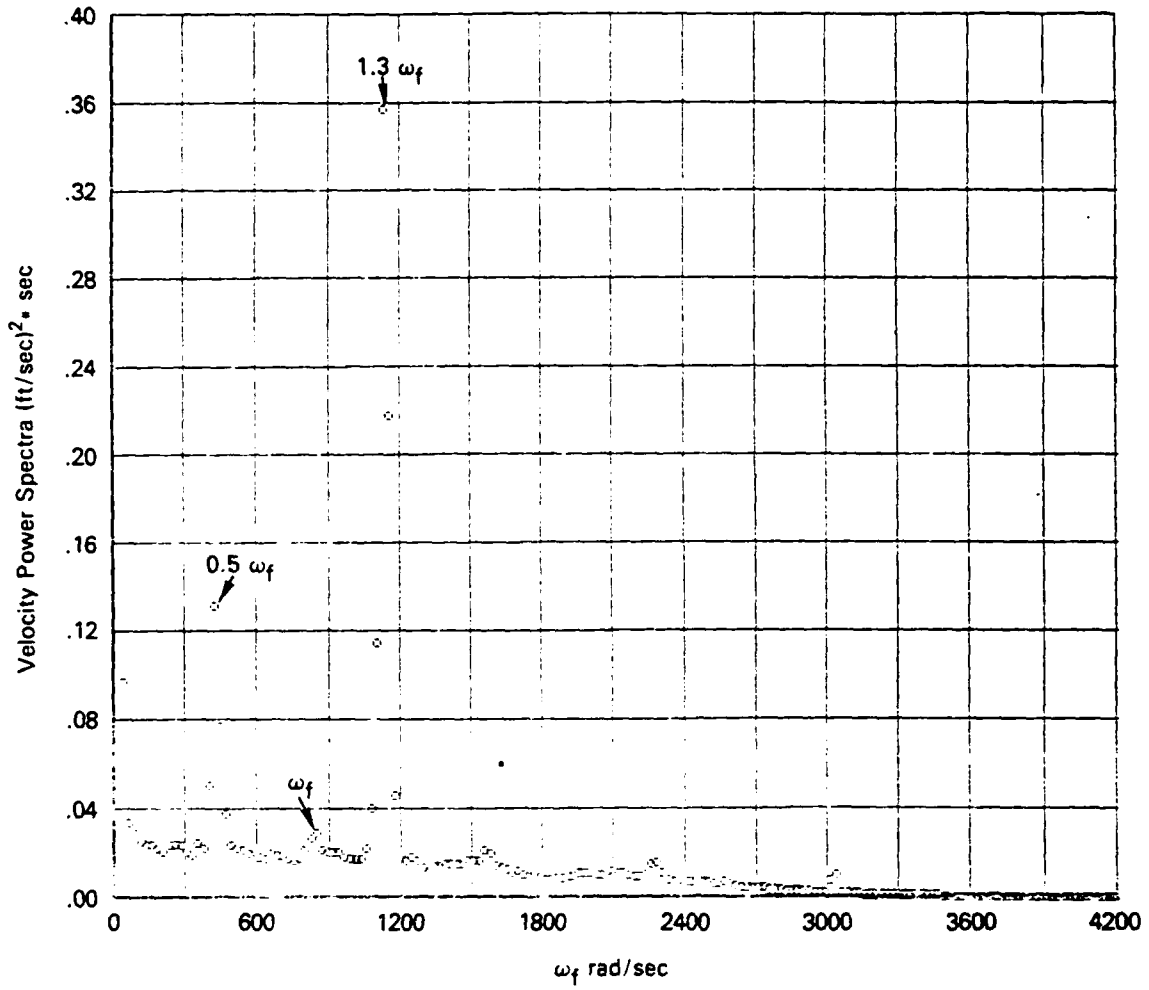


Figure 5 - Power Spectral Density Plot for a Hot Wire Anemometer Signal During a Run with $\omega_v = 0.93$ Hz

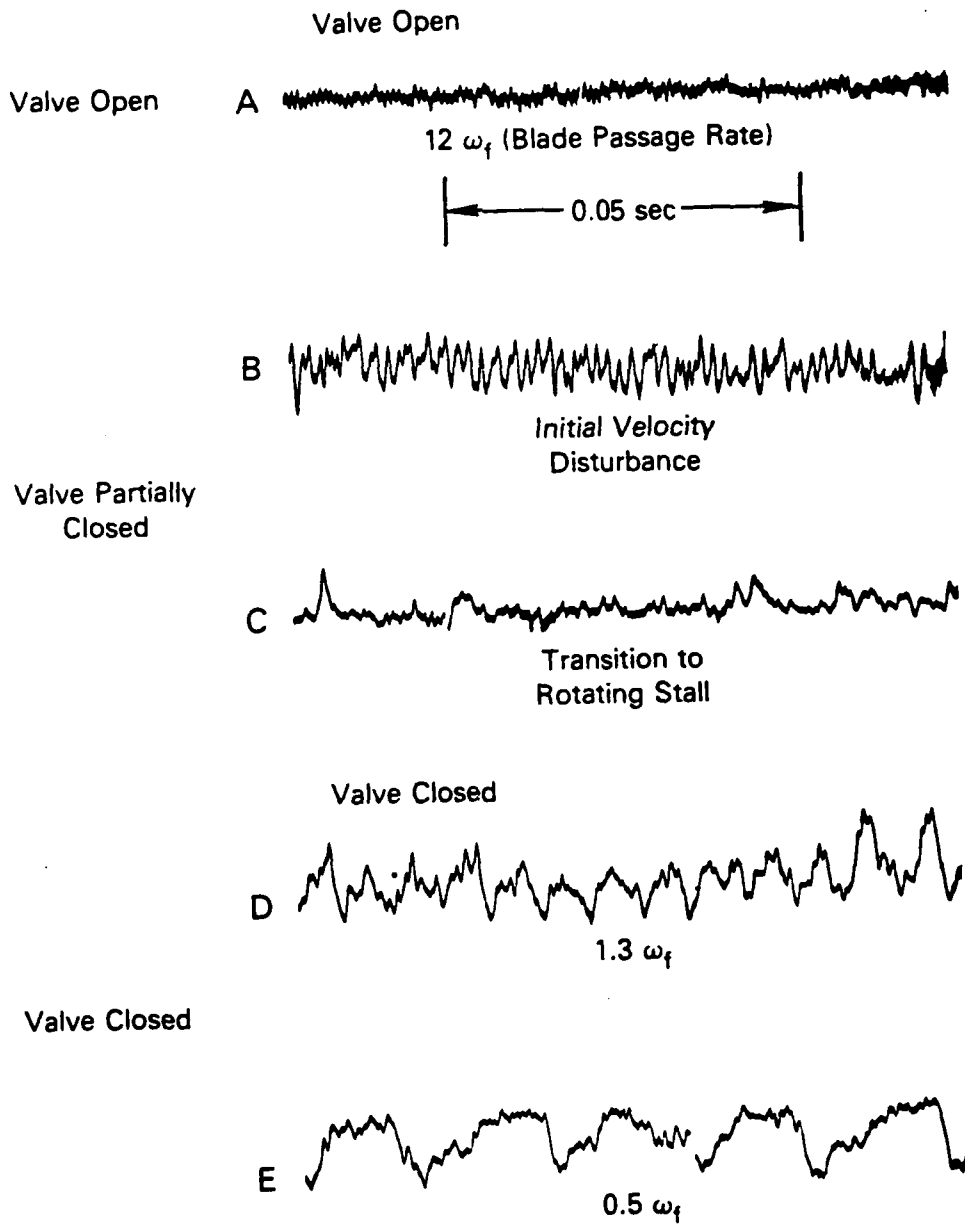


Figure 6 - Detailed Velocity Time History of Portion of a Valve Cycle with $\omega_v = 0.96$ Hz

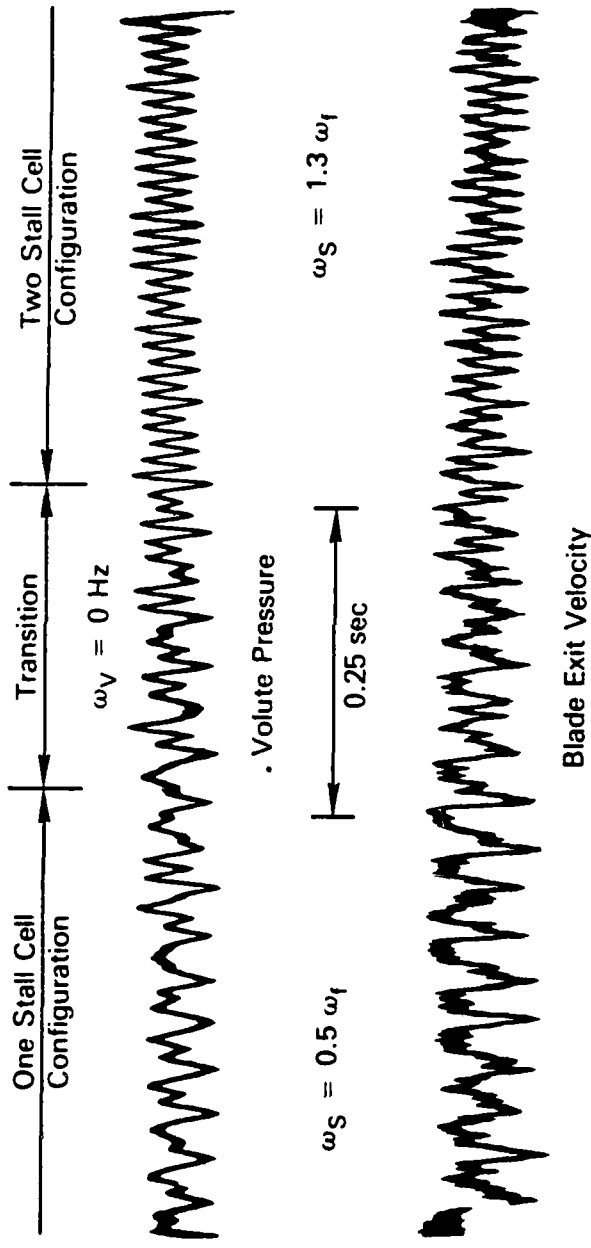


Figure 7 - Transition Between Rotating Stall Configurations for $\omega_v = 0$

INITIAL DISTRIBUTION LIST

	<u>No. of Copies</u>
Defense Documentation Center Cameron Station Alexandria, Virginia 22134	5
Assistant Librarian Technical Processing Division U. S. Naval Academy Annapolic, Maryland 21402	4
Academic Dean U. S. Naval Academy Annapolic, Maryland 21402	1
Director of Research U. S. Naval Academy Annapolic, Maryland 21402	1
Division Director Division of Engineering and Weapons U. S. Naval Academy Annapolic, Maryland 21402	1
Department Chairman Naval Systems Engineering Department U. S. Naval Academy Annapolis, Maryland 21402	2